EUROPEAN LABORATORY FOR PARTICLE PHYSICS

CERN-PPE/97-04
10th January 1997

Measurement of the triple gauge boson coupling $\alpha_{W\phi}$ from W^+W^- production in e^+e^- collisions at $\sqrt{s} = 161$ GeV

The OPAL Collaboration

Abstract

This letter describes a measurement of one of the anomalous triple gauge boson couplings using the first data recorded by the OPAL detector at LEP2. A total of 28 W-pair candidates have been selected for an integrated luminosity of 9.89 ± 0.06 pb^{-1} recorded at a centre-of-mass energy of 161 GeV. We use these data to place constraints upon the coupling parameter $\alpha_{W\phi}$. We analyse the predicted variation of the total cross-section for all observed channels and the distribution of kinematic variables in the semileptonic decay channels. We measure $\alpha_{W\phi}$ to be $-0.61^{+0.73}_{-0.61} \pm 0.35$, which is consistent with the Standard Model expectation of zero.

(Submitted to Physics Letters B)

The OPAL Collaboration

K. Ackerstaff[8], G. Alexander[23], J. Allison[16], N. Altekamp[5], K. Ametewee[25], K.J. Anderson[9], S. Anderson[12], S. Arcelli[2], S. Asai[24], D. Axen[29], G. Azuelos[18,a], A.H. Ball[17], E. Barberio[8], R.J. Barlow[16], R. Bartoldus[3], J.R. Batley[5], J. Bechtluft[14], C. Beeston[16], T. Behnke[8], A.N. Bell[1], K.W. Bell[20], G. Bella[23], S. Bentvelsen[8], P. Berlich[10], S. Bethke[14], O. Biebel[14], S.D. Bird[16], A. Biguzzi[5], V. Blobel[27], I.J. Bloodworth[1], J.E. Bloomer[1], M. Bobinski[10], P. Bock[11], H.M. Bosch[11], M. Boutemeur[34], B.T. Bouwens[12], S. Braibant[12], R.M. Brown[20], H.J. Burckhart[8], C. Burgard[8], R. Bürgin[10], P. Capiluppi[2], R.K. Carnegie[6], A.A. Carter[13], J.R. Carter[5], C.Y. Chang[17], D.G. Charlton[1,b], D. Chrisman[4], P.E.L. Clarke[15], I. Cohen[23], J.E. Conboy[15], O.C. Cooke[16], M. Cuffiani[2], S. Dado[22], C. Dallapiccola[17], G.M. Dallavalle[2], S. De Jong[12], L.A. del Pozo[4], K. Desch[3], M.S. Dixit[7], E. do Couto e Silva[12], M. Doucet[18], E. Duchovni[26], G. Duckeck[34], I.P. Duerdoth[16], D. Eatough[16], J.E.G. Edwards[16], P.G. Estabrooks[6], H.G. Evans[9], M. Evans[13], F. Fabbri[2], M. Fanti[2], P. Fath[11], A.A. Faust[30], F. Fiedler[27], M. Fierro[2], H.M. Fischer[3], R. Folman[26], D.G. Fong[17], M. Foucher[17], A. Fürtjes[8], P. Gagnon[7], J.W. Gary[4], J. Gascon[18], S.M. Gascon-Shotkin[17], N.I. Geddes[20], C. Geich-Gimbel[3], T. Geralis[20], G. Giacomelli[2], P. Giacomelli[4], R. Giacomelli[2], V. Gibson[5], W.R. Gibson[13], D.M. Gingrich[30,a], D. Glenzinski[9], J. Goldberg[22], M.J. Goodrick[5], W. Gorn[4], C. Grandi[2], E. Gross[26], J. Grunhaus[23], M. Gruwé[8], C. Hajdu[32], G.G. Hanson[12], M. Hansroul[8], M. Hapke[13], C.K. Hargrove[7], P.A. Hart[9], C. Hartmann[3], M. Hauschild[8], C.M. Hawkes[5], R. Hawkings[27], R.J. Hemingway[6], M. Herndon[17], G. Herten[10], R.D. Heuer[8], M.D. Hildreth[8], J.C. Hill[5], S.J. Hillier[1], T. Hilse[10], P.R. Hobson[25], R.J. Homer[1], A.K. Honma[28,a], D. Horváth[32,c], R. Howard[29], R.E. Hughes-Jones[16], D.E. Hutchcroft[5], P. Igo-Kemenes[11], D.C. Imrie[25], M.R. Ingram[16], K. Ishii[24], A. Jawahery[17], P.W. Jeffreys[20], H. Jeremie[18], M. Jimack[1], A. Joly[18], C.R. Jones[5], G. Jones[16], M. Jones[6], R.W.L. Jones[8], U. Jost[11], P. Jovanovic[1], T.R. Junk[8], D. Karlen[6], K. Kawagoe[24], T. Kawamoto[24], R.K. Keeler[28], R.G. Kellogg[17], B.W. Kennedy[20], J. Kirk[29], S. Kluth[8], T. Kobayashi[24], M. Kobel[10], D.S. Koetke[6], T.P. Kokott[3], M. Kolrep[10], S. Komamiya[24], T. Kress[11], P. Krieger[6], J. von Krogh[11], P. Kyberd[13], G.D. Lafferty[16], R. Lahmann[17], W.P. Lai[19], D. Lanske[14], J. Lauber[15], S.R. Lautenschlager[31], J.G. Layter[4], D. Lazic[22], A.M. Lee[31], E. Lefebvre[18], D. Lellouch[26], J. Letts[12], L. Levinson[26], C. Lewis[15], S.L. Lloyd[13], F.K. Loebinger[16], G.D. Long[28], M.J. Losty[7], J. Ludwig[10], A. Macchiolo[2], A. Macpherson[30], M. Mannelli[8], S. Marcellini[2], C. Markus[3], A.J. Martin[13], J.P. Martin[18], G. Martinez[17], T. Mashimo[24], W. Matthews[25], P. Mättig[3], W.J. McDonald[30], J. McKenna[29], E.A. Mckigney[15], T.J. McMahon[1], A.I. McNab[13], R.A. McPherson[8], F. Meijers[8], S. Menke[3], F.S. Merritt[9], H. Mes[7], J. Meyer[27], A. Michelini[2], G. Mikenberg[26], D.J. Miller[15], R. Mir[26], W. Mohr[10], A. Montanari[2], T. Mori[24], M. Morii[24], U. Müller[3], K. Nagai[26], I. Nakamura[24], H.A. Neal[8], B. Nellen[3], B. Nijjhar[16], R. Nisius[8], S.W. O'Neale[1], F.G. Oakham[7], F. Odorici[2], H.O. Ogren[12], N.J. Oldershaw[16], T. Omori[24], M.J. Oreglia[9], S. Orito[24], J. Pálinkás[33,d], G. Pásztor[32], J.R. Pater[16], G.N. Patrick[20], J. Patt[10], M.J. Pearce[1], S. Petzold[27], P. Pfeifenschneider[14], J.E. Pilcher[9], J. Pinfold[30], D.E. Plane[8], P. Poffenberger[28], B. Poli[2], A. Posthaus[3], H. Przysiezniak[30], D.L. Rees[1], D. Rigby[1], S. Robertson[28], S.A. Robins[13], N. Rodning[30], J.M. Roney[28], A. Rooke[15], E. Ros[8], A.M. Rossi[2], M. Rosvick[28], P. Routenburg[30], Y. Rozen[22], K. Runge[10], O. Runolfsson[8], U. Ruppel[14], D.R. Rust[12], R. Rylko[25], K. Sachs[10], E.K.G. Sarkisyan[23], M. Sasaki[24], C. Sbarra[29], A.D. Schaile[34], O. Schaile[34], F. Scharf[3], P. Scharff-Hansen[8], P. Schenk[34], B. Schmitt[8], S. Schmitt[11], M. Schröder[8], H.C. Schultz-Coulon[10], M. Schulz[8], M. Schumacher[3], P. Schütz[3], W.G. Scott[20], T.G. Shears[16], B.C. Shen[4], C.H. Shepherd-Themistocleous[8], P. Sherwood[15], G.P. Siroli[2], A. Sittler[27],

A. Skillman[15], A. Skuja[17], A.M. Smith[8], T.J. Smith[28], G.A. Snow[17], R. Sobie[28], S. Söldner-Rembold[10], R.W. Springer[30], M. Sproston[20], A. Stahl[3], M. Steiert[11], K. Stephens[16], J. Steuerer[27], B. Stockhausen[3], D. Strom[19], P. Szymanski[20], R. Tafirout[18], S.D. Talbot[1], S. Tanaka[24], P. Taras[18], S. Tarem[22], M. Thiergen[10], M.A. Thomson[8], E. von Törne[3], S. Towers[6], I. Trigger[18], T. Tsukamoto[24], E. Tsur[23], A.S. Turcot[9], M.F. Turner-Watson[8], P. Utzat[11], R. Van Kooten[12], M. Verzocchi[10], P. Vikas[18], M. Vincter[28], E.H. Vokurka[16], F. Wäckerle[10], A. Wagner[27], C.P. Ward[5], D.R. Ward[5], J.J. Ward[15], P.M. Watkins[1], A.T. Watson[1], N.K. Watson[1], P.S. Wells[8], N. Wermes[3], J.S. White[28], B. Wilkens[10], G.W. Wilson[27], J.A. Wilson[1], G. Wolf[26], S. Wotton[5], T.R. Wyatt[16], S. Yamashita[24], G. Yekutieli[26], V. Zacek[18], D. Zer-Zion[8]

[1]School of Physics and Space Research, University of Birmingham, Birmingham B15 2TT, UK
[2]Dipartimento di Fisica dell' Università di Bologna and INFN, I-40126 Bologna, Italy
[3]Physikalisches Institut, Universität Bonn, D-53115 Bonn, Germany
[4]Department of Physics, University of California, Riverside CA 92521, USA
[5]Cavendish Laboratory, Cambridge CB3 0HE, UK
[6] Ottawa-Carleton Institute for Physics, Department of Physics, Carleton University, Ottawa, Ontario K1S 5B6, Canada
[7]Centre for Research in Particle Physics, Carleton University, Ottawa, Ontario K1S 5B6, Canada
[8]CERN, European Organisation for Particle Physics, CH-1211 Geneva 23, Switzerland
[9]Enrico Fermi Institute and Department of Physics, University of Chicago, Chicago IL 60637, USA
[10]Fakultät für Physik, Albert Ludwigs Universität, D-79104 Freiburg, Germany
[11]Physikalisches Institut, Universität Heidelberg, D-69120 Heidelberg, Germany
[12]Indiana University, Department of Physics, Swain Hall West 117, Bloomington IN 47405, USA
[13]Queen Mary and Westfield College, University of London, London E1 4NS, UK
[14]Technische Hochschule Aachen, III Physikalisches Institut, Sommerfeldstrasse 26-28, D-52056 Aachen, Germany
[15]University College London, London WC1E 6BT, UK
[16]Department of Physics, Schuster Laboratory, The University, Manchester M13 9PL, UK
[17]Department of Physics, University of Maryland, College Park, MD 20742, USA
[18]Laboratoire de Physique Nucléaire, Université de Montréal, Montréal, Quebec H3C 3J7, Canada
[19]University of Oregon, Department of Physics, Eugene OR 97403, USA
[20]Rutherford Appleton Laboratory, Chilton, Didcot, Oxfordshire OX11 0QX, UK
[22]Department of Physics, Technion-Israel Institute of Technology, Haifa 32000, Israel
[23]Department of Physics and Astronomy, Tel Aviv University, Tel Aviv 69978, Israel
[24]International Centre for Elementary Particle Physics and Department of Physics, University of Tokyo, Tokyo 113, and Kobe University, Kobe 657, Japan
[25]Brunel University, Uxbridge, Middlesex UB8 3PH, UK
[26]Particle Physics Department, Weizmann Institute of Science, Rehovot 76100, Israel
[27]Universität Hamburg/DESY, II Institut für Experimental Physik, Notkestrasse 85, D-22607 Hamburg, Germany
[28]University of Victoria, Department of Physics, P O Box 3055, Victoria BC V8W 3P6, Canada

[29]University of British Columbia, Department of Physics, Vancouver BC V6T 1Z1, Canada
[30]University of Alberta, Department of Physics, Edmonton AB T6G 2J1, Canada
[31]Duke University, Dept of Physics, Durham, NC 27708-0305, USA
[32]Research Institute for Particle and Nuclear Physics, H-1525 Budapest, P O Box 49, Hungary
[33]Institute of Nuclear Research, H-4001 Debrecen, P O Box 51, Hungary
[34]Ludwigs-Maximilians-Universität München, Sektion Physik, Am Coulombwall 1, D-85748 Garching, Germany

[a] and at TRIUMF, Vancouver, Canada V6T 2A3
[b] and Royal Society University Research Fellow
[c] and Institute of Nuclear Research, Debrecen, Hungary
[d] and Department of Experimental Physics, Lajos Kossuth University, Debrecen, Hungary

1 Introduction

In the initial phase of operation of LEP2, centre-of-mass energies of $\sqrt{s} = 161$ GeV have been attained, allowing the production of W^+W^- boson pairs for the first time in e^+e^- collisions. The W^+W^- production process involves the triple gauge boson vertices between the W^+W^- and the Z^0 or photon. The measurement of these triple gauge boson couplings (TGCs) and the search for possible anomalous values is one of the principal physics goals at LEP2. The observable effects of such deviations have been studied extensively [1]. Anomalous TGCs can affect both the total production cross-section and the shape of the differential cross-section as a function of the W^- production angle. The relative contributions of each helicity state of the W bosons are also changed, which in turn affects the distributions of their decay products.

Anomalous TGCs are associated with contributions to W^+W^- production that rise with $\sqrt{s}$ and which would lead to violation of unitarity. Measurements at $\sqrt{s} = 161$ GeV are therefore somewhat less sensitive to TGCs than the measurements which will be possible at higher energies. A further effect at the W^+W^- threshold is that the s-channel triple gauge boson diagrams are suppressed at tree level relative to the dominant t-channel neutrino exchange diagram by a factor of $\beta^2 = 1 - 4{M_W}^2/s$. However due to the width of the W the sensitivity at threshold is enhanced relative to this simple expectation. The first reason for this is that the W bosons can be off-shell and their average β is increased. This alone leads to a significant enhancement of the s-channel diagrams. Secondly the increase in β results in an increase in the average W momentum and the measurement of this quantity is sensitive to anomalous TGCs.

In this letter we use the first sample of $e^+e^- \rightarrow W^+W^-$ pair threshold production data accumulated by the OPAL detector. We use these data to place constraints upon one of the models adopted during the LEP2 workshop [1], the so called $W\phi$ model. We present an analysis of the total production cross-section measured using all observed events and of the W momentum spectrum and angular distributions measured using the semileptonic decay channels.

The $W\phi$ model

The most general Lorentz invariant Lagrangian [1] which describes the triple gauge boson interaction has up to fourteen independent terms, seven describing the WWγ vertex and seven describing the WWZ vertex. This parameter space is very large, and it is not currently possible to measure all parameters independently. Assuming electromagnetic gauge invariance and C and P conservation this parameter set reduces to five, which we can write as $g_1^z, \kappa_z, \kappa_\gamma, \lambda_z$ and λ_γ following the notation used in [1, 2]. In the Standard Model $g_1^z = \kappa_z = \kappa_\gamma = 1$ and $\lambda_z = \lambda_\gamma = 0$. Triple gauge boson couplings contribute through virtual corrections to many observables measured at lower energies and the precise measurements at LEP1 allow constraints to be placed upon the parameter space of these five quantities [3]. As a result three specific linear combinations of these couplings have been proposed [1, 2, 4] which are not tightly constrained by LEP1 data. These are:

$$\begin{aligned} \alpha_{B\phi} &\equiv \Delta\kappa_\gamma - \Delta g_1^z \cos^2\theta_w \\ \alpha_{W\phi} &\equiv \Delta g_1^z \cos^2\theta_w \end{aligned}$$

$$\alpha_W \equiv \lambda_\gamma$$

with the constraints that $\Delta\kappa_z = -\Delta\kappa_\gamma \tan^2\theta_w + \Delta g_1^z$ and $\lambda_z = \lambda_\gamma$. The Δ indicates the deviation of the respective quantity from unity and θ_w is the weak mixing angle. In this analysis we measure the $\alpha_{W\phi}$ coupling assuming $\alpha_{B\phi}$ and α_W to be zero. This means that we allow only $\Delta\kappa_\gamma, \Delta\kappa_z$ and Δg_1^z to vary from zero under the constraints that $\Delta g_1^z \cos^2\theta_w = \Delta\kappa_\gamma$ and that $\Delta\kappa_z$ is as given above.

2 Data selection and simulated event samples

The data were recorded during 1996 at $\sqrt{s} = 161.3 \pm 0.2$ GeV [5] using the OPAL detector, which is fully described elsewhere [6, 7]. A total integrated luminosity of 9.89 pb^{-1} was recorded at this energy. The selection and reconstruction of W^+W^- events produced by the reaction $e^+e^- \to W^+W^-$ has been described in [8], which includes a description of lepton identification and jet finding. Events are selected based upon five different W pair decay combinations. These are: $q\bar{q}q\bar{q}$ events where both W bosons decay to a two-jet final state, semileptonic $q\bar{q}\ell\bar{\nu}_\ell$ events where one W decays to a two-jet final state, and the other W decays to an electron, muon or tau, plus a neutrino and $\ell^-\bar{\nu}_\ell\ell'^+\nu_{\ell'}$ events where both W bosons decay to a lepton plus a neutrino. A total of 28 events were selected with an expected background of 5.0 ± 0.6 events.

For the analysis of the kinematic distributions in the $q\bar{q}\ell\bar{\nu}_\ell$ channels we have augmented the selections of [8] in order to reduce further the contamination from single $Z^0 \to q\bar{q}$ or $\gamma \to q\bar{q}$ events. In the selection of [8] a single high momentum lepton and exactly two hadronic jets are required. The jets are formed from the tracks and calorimeter clusters of the hadronic system using the $k_\perp$ ("Durham") [9] algorithm, and the total energy and momentum of each of the jets are corrected for double counting of energy [10]. The missing energy and momentum of the event are assigned to the neutrino. In this analysis we add the following requirements. In the $q\bar{q}e\bar{\nu}_e$ and $q\bar{q}\mu\bar{\nu}_\mu$ channels we apply a two dimensional cut in the plane of the invariant masses of the $q\bar{q}$ and $\ell\bar{\nu}_\ell$ systems, $M_{l\nu}$ and $M_{q\bar{q}}$. The selection requires that $M_{q\bar{q}} < 30$ GeV $+ 1.65\ M_{l\nu}$ and $M_{q\bar{q}} > 135$ GeV $- M_{l\nu}$. In the $q\bar{q}\tau\bar{\nu}_\tau$ channel the cut on the cosine of the angle between the missing momentum vector and the beam direction is tightened to $|\cos\theta_{miss}| < 0.8$ and two further cuts are applied. The invariant mass of the hadronic system, $M_{q\bar{q}}$ is required to satisfy 40 GeV $< M_{q\bar{q}} <$ 90 GeV and the cosine of the angle between the τ jet direction and the missing momentum vector is required to be less than zero.

Details of the resulting signal, efficiencies, and background[1] contaminations are shown in tables 1 and 2. These are obtained using the same procedures as detailed in [8]. In comparison to the selections of [8] the $Z^0/\gamma \to q\bar{q}$ background is reduced from 5.7% to 1.0% and 1.8% to 0.8% in the e and μ channels, respectively. The number of events selected from the data does not change. In the $q\bar{q}\tau\bar{\nu}_\tau$ channel the background contamination from $Z^0/\gamma \to q\bar{q}$ events is reduced from 22% to 10% and the number of events selected is reduced from seven to six.

[1] In table 2 the cross contamination between $q\bar{q}\ell\bar{\nu}_\ell$ channels is shown. In particular there is a 16% contamination from $q\bar{q}e\bar{\nu}_e$ and $q\bar{q}\mu\bar{\nu}_\mu$ events to the $q\bar{q}\tau\bar{\nu}_\tau$ channel. However it should be noted that no attempt has been made to try to reject these in the selection procedure. This is because due to our method of τ reconstruction the e and μ contamination to τ's is effectively considered as signal.

We use Monte Carlo samples to provide predictions of quantities as a function of $\alpha_{W\phi}$. The principal Standard Model sample is obtained using PYTHIA [11] and is generated using the current world average W boson mass of $M_{\mathrm{W}} = 80.33 \pm 0.15$ GeV [12]. The $\mathrm{W^+W^-}$ cross-section for this sample is within 2% of that predicted by the GENTLE program [13]. To obtain samples corresponding to different anomalous values of $\alpha_{W\phi}$ we use EXCALIBUR [14] generating W pair diagrams only. Estimates of the different background processes are based primarily on the PYTHIA, EXCALIBUR and grc4f [15] generators. KORALW [16] is used in the estimation of systematic uncertainties. All events are passed through the full OPAL simulation program [17] and then subjected to the same reconstruction procedures as applied to the data.

3 Kinematic variables for the $\mathrm{q\bar{q}}\ell\bar{\nu}_\ell$ event sample

The $\mathrm{q\bar{q}}\ell\bar{\nu}_\ell$ events are the most straightforward to reconstruct since there is no ambiguity in assigning decay fermion pairs to each W nor in determining the charges of each W. In contrast the $\mathrm{q\bar{q}q\bar{q}}$ channel has both of these problems and a higher background, leading to a much reduced sensitivity to TGCs. Therefore in this analysis we analyse the kinematic distributions only in the $\mathrm{q\bar{q}}\ell\bar{\nu}_\ell$ channels.

For each $\mathrm{q\bar{q}}\ell\bar{\nu}_\ell$ event we measure four variables:

1) $\cos\theta_{\mathrm{W}}$, the production angle of the $\mathrm{W^-}$ with respect to the $\mathrm{e^-}$ beam direction,

2) p_{W}, the momentum of the hadronically decaying W,

3) $\cos\theta^*_\ell$, the polar decay angle of the charged lepton with respect to the W flight direction measured in the W rest frame and

4) ϕ^*_ℓ, the azimuthal decay angle of the charged lepton with respect to a plane defined by the W and the beam axis.

The exact definition of the decay angles is described in [1, 2, 18]. We do not distinguish the charges of the quarks from the hadronically decaying W. As a result the decay angles of the quarks can only be determined with a two fold ambiguity which substantially reduces their sensitivity to TGCs. We therefore do not use these angles in this analysis.

$\mathrm{q\bar{q}e\bar{\nu}_e}$ and $\mathrm{q\bar{q}}\mu\bar{\nu}_\mu$ events

In the case of $\mathrm{q\bar{q}e\bar{\nu}_e}$ and $\mathrm{q\bar{q}}\mu\bar{\nu}_\mu$ events we use variables resulting from a kinematic fit. This fit demands energy and momentum conservation and a zero mass for the missing neutrino, resulting in one constraint. As input to the fit we use the electron momentum constructed from the direction measured by the tracking detectors and the energy measured in the electromagnetic calorimeters (except for an overlap region between the barrel and endcap in which case the measured track momentum is used instead). In the case of muons we use the momentum measured using the tracking detectors. We neglect initial state radiation when applying energy

and momentum conservation in the reconstruction. However in the analysis we compare the data with Monte Carlo distributions which are subject to exactly the same reconstruction procedure and which include ISR in the simulation. Therefore the method compares like with like and should introduce no bias. This has been explicitly checked and at the present level of statistical accuracy any residual bias has been found to be negligible.

We obtain $\cos\theta_{\mathrm{W}}$ and p_{W} by adding together the fitted four-momenta of the two jets. The charges of the W bosons are determined by the sign of the charged lepton. The lepton decay angles are obtained by boosting the fitted lepton four-vectors to the parent W rest frame, and using the definitions given in the references above. The predicted resolution of each of these quantities obtained from Monte Carlo events is shown in figure 1.

$\mathrm{q\bar{q}}\tau\bar{\nu}_\tau$ events

The $\mathrm{q\bar{q}}\tau\bar{\nu}_\tau$ selection procedure results in three jet events, where one jet has been identified as a tau jet containing one or three tracks. From Monte Carlo studies this is found to make the correct selection of the tau in more than 97% of cases.

We obtain $\cos\theta_{\mathrm{W}}$ and p_{W} by adding together the measured four-momenta of the two jets. The charges of the W bosons are determined by the sign of the sum of the charges of the tracks in the τ jet. This yields the correct charge in 98% of the events where the τ has been correctly identified.

In order to reconstruct the decay angles, the flight direction of the τ is approximated by the direction of its jet. The four unknown quantities can then be calculated using energy and momentum conservation. These are the energy of the τ and the three-momentum of the τ neutrino originating directly from the W decay. The decay angles are then obtained as for the other $\mathrm{q\bar{q}}\ell\bar{\nu}_\ell$ events. The predicted resolutions for these quantities do not differ significantly from the resolutions obtained in the other $\mathrm{q\bar{q}}\ell\bar{\nu}_\ell$ channels and are shown in fig 1. The reason for this is that reconstruction of all variables depends mainly upon the hadronic system.

In figure 2 we show the distributions of all quantities obtained from the 11 $\mathrm{q\bar{q}e\bar{\nu}_e}$, $\mathrm{q\bar{q}}\mu\bar{\nu}_\mu$ and $\mathrm{q\bar{q}}\tau\bar{\nu}_\tau$ events added together. They are compared with the distributions expected in the Standard Model using fully simulated Monte Carlo events.

4 $\alpha_{W\phi}$ analysis

In this section we analyse the $\mathrm{W^+W^-}$ event sample in order to place limits upon $\alpha_{W\phi}$. We do this in two parts. In the first part we calculate the log likelihood ($\log\mathcal{L}$) for observing the 28 events in our data sample as a function of $\alpha_{W\phi}$. In the second part we calculate the $\log\mathcal{L}$ for the 11 $\mathrm{q\bar{q}}\ell\bar{\nu}_\ell$ events to have their measured distribution of kinematic variables, as a function of $\alpha_{W\phi}$. These likelihoods are independent and we add them to give the overall $\log\mathcal{L}$ distribution from which we derive the results.

4.1 Analysis of the total number of observed events

In this part of the analysis all channels are combined. The W^+W^- production cross-section varies with $\alpha_{W\phi}$, having a minimum near the Standard Model value of zero and increasing parabolically for $\alpha_{W\phi} \neq 0$. For each assumed value of $\alpha_{W\phi}$ we calculate the likelihood for the expected mean number of events to have resulted in our observed number of 28 events.

The expected mean number of signal events as a function of $\alpha_{W\phi}$ is obtained by multiplying the expected cross-section by the recorded integrated luminosity value of 9.89 ± 0.06 pb^{-1}. To calculate the expected cross-section we take advantage of the fact that this is a quadratic function of any TGC parameter. Five EXCALIBUR Monte Carlo samples with $\alpha_{W\phi} = -2, -1, 0, 1, 2$ were passed through the same selection requirements as the real data and the accepted cross-section found for all channels combined. All five points were found to lie on a parabola and this was parameterised and used to predict the cross-section for all other values of $\alpha_{W\phi}$. We use the W mass value of 80.33 ± 0.15 GeV [12] which excludes the recent LEP results. The LEP beam energy is taken to be 80.65 ± 0.10 GeV [5]. The EXCALIBUR cross-sections are multiplied by a factor of 1.026 ± 0.026 to account for the slight difference [8] between EXCALIBUR and GENTLE, as the latter is more complete [19].

The probability of finding the observed number of events was calculated assuming a Poisson distribution for the signal and background. The negative $\log \mathcal{L}$ distribution obtained from this procedure is shown in figure 3.

4.2 Analysis of the differential distributions

In the second part of this analysis a binned likelihood method is used to analyse the $\cos\theta_W$, p_W, $\cos\theta^*_\ell$ and ϕ^*_ℓ distributions. As discussed in the introduction each of these variables depends upon $\alpha_{W\phi}$. This is illustrated in figure 2, which shows the distributions of each, integrated over the other three variables, for our data sample and three Monte Carlo samples with $\alpha_{W\phi} = -2, 0, 2$.

In this analysis p_W is divided into three bins in the range [0,45] GeV, $\cos\theta_W$ and $\cos\theta^*_\ell$ are divided into five bins in the range $[-1,1]$ and ϕ^*_ℓ is divided into five bins in the range $[-\pi, \pi]$, giving a total of 375 bins which we label i. The $\log \mathcal{L}$ distribution is obtained in several steps.

In the first step we parameterise in each bin the expected cross-section, before detector and acceptance effects, as a function of $\alpha_{W\phi}$. We denote this as $\sigma_i^{gen}(\alpha_{W\phi})$. It is obtained using large samples of Monte Carlo events without detector simulation. In each bin $\sigma_i^{gen}(\alpha_{W\phi})$ is parameterised using the quadratic dependence upon $\alpha_{W\phi}$.

In the second step we calculate correction factors to include the effects of acceptance, resolution and the contribution of other W^+W^- decay channels to the sample. We use fully simulated Monte Carlo events generated with $\alpha_{W\phi} = 0$ to obtain the factors, c_{ki}, which allow for events generated in true bin i being reconstructed in bin k. All W^+W^- decays are included in the sample and all events which are reconstructed as $q\bar{q}\ell\bar{\nu}_\ell$ events in bin k are counted in the correction factors c_{ki}. For a given bin, corresponding to a limited phase space region,

these effects do not depend strongly on $\alpha_{W\phi}$. The c_{ki} factors are therefore assumed to be independent of $\alpha_{W\phi}$. It has been explicitly checked that no significant bias is introduced by this approximation.

Combining these terms results in the expected observed cross-section for each bin k, due to all $\mathrm{W^+W^-}$ channels:

$$\sigma_k^{\mathrm{WW}}(\alpha_{W\phi}) = \sum_i c_{ki}\sigma_i^{gen}(\alpha_{W\phi})$$

In the next step the cross-section for non-$\mathrm{W^+W^-}$ background sources, σ_k^{bkg}, is estimated from the corresponding Monte Carlo samples. The variation with $\alpha_{W\phi}$ of the contribution to σ_k^{bkg} from Weν events is considered in the systematic checks. The background cross section is added to give $\sigma_k^{all}(\alpha_{W\phi})$:

$$\sigma_k^{all}(\alpha_{W\phi}) = \sigma_k^{\mathrm{WW}}(\alpha_{W\phi}) + \sigma_k^{bkg}$$

This expression now contains all of the information on the shape of the expected distribution in the four-dimensional space, as a function of $\alpha_{W\phi}$. We multiply this by a scale factor to give the prediction for the number of events in each bin, n_k, where the scale factor is chosen such that the predicted total number of events is equal to the actual number of events observed in the data. This is to ensure that we do not incorporate any overall cross-section information in this part of the analysis.

Finally the probability for observing the number of events seen in each bin for an expectation of n_k is calculated using Poisson statistics. The statistical fluctuations in c_{ki} and σ_k^{bkg} are taken into account using the method of reference [20]. The negative $\log\mathcal{L}$ distribution for the data set is shown in figure 3.

In order to check the possible bias in the method, it was tested using different samples of Monte Carlo events taken as data events. These samples with values of $\alpha_{W\phi}$ ranging between -2 and 2 were passed through the full detector simulation. Each sample had 1500 events after selection cuts. The resulting fitted values for $\alpha_{W\phi}$ were always consistent with the input values.

We have also checked these results using two independent analyses. In the first method an unbinned likelihood analysis was developed to analyse only $\mathrm{d}\sigma/\mathrm{d}\cos\theta_{\mathrm{W}}$. In the second method the entire analysis was formulated using optimal observables [1, 21]. The measured optimal observable corresponding to $\alpha_{W\phi}$ was compared with the predicted value as a function of $\alpha_{W\phi}$ and the likelihood calculated. In all cases the $\log\mathcal{L}$ distributions were found to be consistent with the binned method applied to the corresponding observables.

4.3 Combined analysis

The individual $\log\mathcal{L}$ distributions shown in figure 3 are compatible with the same minimum point. These are independent measurements and therefore have been added together to give the overall $\log\mathcal{L}$ distribution shown as the solid line in the figure.

We can express this as a measurement with the one standard deviation limits given by the values of $\alpha_{W\phi}$ where $\Delta\log\mathcal{L} = 0.5$. This yields the result $\alpha_{W\phi} = -0.61^{+0.73}_{-0.61}$, where only

the statistical error is included. The expected error for a sample of this size was evaluated by repeating the analysis using Monte Carlo events divided into sub-samples equivalent to the actual data sample. We find an expected statistical error of ± 0.68.

To express this as a 95% confidence level (C.L.) limit we take the points of intersection of the curve with the $\Delta \log \mathcal{L} = 1.92$ line. This yields the result: $-1.74 < \alpha_{W\phi} < 0.94$ at 95% C.L., where again only the statistical error is included in this range. It should be noted that the $\log \mathcal{L}$ distribution is not parabolic and therefore different C.L. ranges cannot be obtained simply from the one standard deviation values, but have to be determined directly from the distribution.

5 Systematic studies

The Monte Carlo simulation of the measured quantities depends mainly upon the simulation of the jets from the W hadronic decay. Jet reconstruction has been studied and tuned extensively at LEP1, showing good agreement between distributions measured from data and Monte Carlo samples. We therefore expect this to be adequate for the small number of events in this sample.

As a direct test of $\cos\theta_{\mathrm{W}}$ reconstruction we have used radiative Z events taken from the $\sqrt{s} = 91$ GeV data. By selecting events containing observed radiated photons with energies up to 20 GeV we obtain a sample of jet pairs exhibiting a similar acollinearity distribution to W decays. Assuming that no other photons have been radiated in the event the true direction of the $\mathrm{Z}^0 \rightarrow \mathrm{q\overline{q}}$ system is opposite to that of the photon. The difference between the value of $\cos\theta$ measured from the photon and that measured from the hadronic system is therefore strongly related to the true resolution of $\cos\theta_{\mathrm{W}}$. The results obtained from both data and Monte Carlo events agree well showing no significant differences in shape or width of the distributions.

In order to quantify reasonable variations of jet reconstruction parameters we have used a sample of radiative Z/γ events selected from the $\sqrt{s} = 161$ GeV data by requiring acollinear two jet events. The invariant mass distribution of the two jets is compared between data and Monte Carlo and a χ^2 is formed for the match. The jet energy scale and resolution for the Monte Carlo events are then artificially varied in order to minimise the χ^2. The best fit variations were then used to vary the Monte Carlo jet reconstruction in the $\alpha_{W\phi}$ analysis and the resulting changes caused to $\alpha_{W\phi}$ were added in quadrature and taken as a systematic error (0.16).

We have evaluated the systematic errors due to Monte Carlo statistics (0.04), the uncertainty in the measured W mass and the LEP beam energy (0.24) and the uncertainties of the overall selection efficiency, background and luminosity measurements (0.06). We have varied the Monte Carlo generator to use both EXCALIBUR and KORALW to generate the Standard Model sample, resulting in a change of 0.10 to $\alpha_{W\phi}$. Since the shape of the distributions is important, regions where the efficiency changes rapidly were excluded and the analysis repeated. This procedure removed at most two events and caused a change of 0.15 to $\alpha_{W\phi}$. We have studied the effect of both doubling the background and setting it to zero (0.02). We have also considered the variation with $\alpha_{W\phi}$ of the background due to Weν events. The accepted cross-section for this process increases by a factor of approximately six for $|\alpha_{W\phi}| \sim 2$. Allowing for this in the analysis caused a negligible change to $\alpha_{W\phi}$. The error due to all sources is listed in table 3.

To obtain the final 95% C.L. limits we have performed a similar procedure. The shift in the 95% upper and lower limits were obtained for each of the variations described above. These shifts were added in quadrature to obtain overall errors for both limits. The upper limit error was added linearly and the lower limit error was subtracted linearly to obtain the final limits.

6 Result and conclusion

Adding the total systematic errors in quadrature we obtain the result

$$\alpha_{W\phi} = -0.61^{+0.73}_{-0.61} \pm 0.35$$

and the corresponding 95% C.L. is

$$-2.1 < \alpha_{W\phi} < 1.6$$

Other experiments at the Tevatron, CDF [22] and D0 [23], have previously reported limits on anomalous TGCs involving the WWZ coupling. However the constraints used in those publications are different to those of this analysis and the results are therefore not directly comparable. To allow an approximate comparison we have repeated our analysis using their sets of constraints but without detector simulation. We find statistical errors from this analysis which are approximately a factor of two greater than the CDF and D0 results.

To give an indication for the implication of this limit we use the unitarity relationship given in [1] $|\alpha_{W\phi}| \sim 15.5(M_{\mathrm{W}}/\Lambda_U)^2$ where Λ_U is the scale at which unitarity would be violated. Assuming this approximate relation our 95% C.L. upper limit corresponds to $\Lambda_U \gtrsim 220$ GeV from this measurement alone.

Acknowledgements

We particularly wish to thank the SL Division for the efficient operation of the LEP accelerator at the new energy of $\sqrt{s} = 161$ GeV and for their continuing close cooperation with our experimental group. We thank our colleagues from CEA, DAPNIA/SPP, CE-Saclay for their efforts over the years on the time-of-flight and trigger systems which we continue to use. In addition to the support staff at our own institutions we are pleased to acknowledge the
Department of Energy, USA,
National Science Foundation, USA,
Particle Physics and Astronomy Research Council, UK,
Natural Sciences and Engineering Research Council, Canada,
Israel Science Foundation, administered by the Israel Academy of Science and Humanities,
Minerva Gesellschaft,

Japanese Ministry of Education, Science and Culture (the Monbusho) and a grant under the Monbusho International Science Research Program,
German Israeli Bi-national Science Foundation (GIF),
Bundesministerium für Bildung, Wissenschaft, Forschung und Technologie, Germany,
National Research Council of Canada,
Hungarian Foundation for Scientific Research, OTKA T-016660, and OTKA F-015089.

References

[1] Physics at LEP2, Edited by G. Altarelli, T. Sjostrand and F. Zwirner, Report on the LEP2 workshop 1995, CERN 96-01 (1996) Vol 1 p525.

[2] M. Bilenky, J.L. Kneur, F.M. Renard and D. Schildknecht, Nucl. Phys. **B409** (1993) 22.

[3] A. De Rujula, M.B. Gavela, P. Hernandez and E. Masso, Nucl. Phys. **B384** (1992) 3, K. Hagiwara, S. Ishihara. R. Szalapski and D. Zeppenfeld, Phys. Lett. **B283** (1992) 353, Phys. Rev. **D48** (1993) 2182.

[4] K. Hagiwara, R.D. Peccei, D. Zeppenfeld, K. Hikasa, Nucl. Phys. **B282** (1987) 253, M. Bilenky, J.L. Kneur, F.M. Renard and D. Schildknecht, Nucl. Phys. **B419** (1994) 240.

[5] LEP Energy Working Group, private communication.

[6] The OPAL Collaboration, K. Ahmet *et al.*, Nucl. Instr. Meth. **A305** (1991) 275, P.P. Allport *et al.*, Nucl. Instr. Meth. **A324** (1993) 34, P.P. Allport *et al.*, Nucl. Instr. Meth. **A346** (1994) 476.

[7] B.E. Anderson *et al.*, IEEE Transactions on Nuclear Science, **41** (1994) 845.

[8] The OPAL Collaboration, K. Ackerstaff *et al.*, 16th October 1996, Phys. Lett. **B389** (1996) 416.

[9] N. Brown and W.J. Stirling, Phys. Lett. **B252** (1990) 657; S. Bethke, Z. Kunszt, D. Soper and W.J. Stirling, Nucl. Phys. **B370** (1992) 310; S. Catani *et al.*, Phys. Lett. **B269** (1991) 432; N. Brown and W.J. Stirling, Zeit. Phys. **C53** (1992) 629.

[10] The OPAL Collaboration, M.Z. Akrawy *et al.*, Phys. Lett. **B253** (1990) 511.

[11] T.Sjöstrand, Comp. Phys. Comm. **82** (1994) 74.

[12] The Particle Data Group, R.M. Barnett *et al.*, Phys. Rev. **D54** (1996) 1, CDF Collaboration, F. Abe *et al.*, Phys. Rev. Lett. **75** (1995) 11, Phys. Rev. **D52** (1995) 4784, CDF Collaboration, F. Abe *et al.*, Phys. Rev. Lett. **65** (1990) 2243, Phys. Rev. **D43** (1991) 2070, UA2 Collaboration, J. Alitti *et al.*, Phys. Lett. **B276** (1992) 354, UA1 Collaboration, C. Albajar *et al.*, Zeit. Phys. **C44** (1989) 15.

[13] D. Bardin *et al.*, Nucl. Phys. B, Proc. Suppl. **37B** (1994) 148-157.

[14] F.A.Berends, R.Pittau and R.Kleiss, Comp. Phys. Comm. **85** (1995) 437, F.A.Berends and A.I. van Sighem, Nucl. Phys. **B454** (1995) 467.

[15] J. Fujimoto *et al.*, KEK-CP-046, hep-ph/9603394, to be published in Comp. Phys. Comm.

[16] M. Skrzypek *et al.*, Comp. Phys. Comm. **94** (1996) 216, M. Skrzypek *et al.*, Phys. Lett. **B372** (1996) 289.

[17] J. Allison *et al.*, Nucl. Instr. Meth. **A317** (1992) 47.

[18] R.L. Sekulin, Phys. Lett. **B338** (1994) 369.

[19] Physics at LEP2, Edited by G. Altarelli, T. Sjostrand and F. Zwirner, Report on the LEP2 workshop 1995, CERN 96-01 (1996) Vol 2 p3.

[20] R. Barlow and C. Beeston, Comp. Phys. Comm. **82** (1994) 74.

[21] M. Diehl, O. Nachtmann, Zeit. Phys. **C62** (1994) 397.

[22] The CDF Collaboration, F. Abe *et al.*, Phys. Rev. Lett. **75** (1995) 1017.

[23] The D0 Collaboration, S. Abachi *et al.*, Phys. Rev. Lett. **75** (1995) 1023,
S. Abachi *et al.*, Phys. Rev. Lett. **77** (1996) 3303.

Channel	Efficiency (%)	Selected events	Predicted	
			signal	background
$q\bar{q}e\bar{\nu}_e$	70 ± 3	3	3.8 ± 0.4	0.2 ± 0.3
$q\bar{q}\mu\bar{\nu}_\mu$	73 ± 3	2	4.0 ± 0.5	0.3 ± 0.2
$q\bar{q}\tau\bar{\nu}_\tau$	29 ± 3	6	1.6 ± 0.2	0.5 ± 0.2

Table 1: The selected number of events in the lepton channels after the additional cuts described in the text. The Standard Model expectation for the numbers of signal and background events are also shown.

	Background contamination %						
	$Z\gamma$	$W^+W^- \to q\bar{q}\ell\bar{\nu}_\ell$	Other W^+W^-	ZZ	Weν	Zee	Total
$q\bar{q}e\bar{\nu}_e$	1.0	3.1	0.1	0.4	0.3	0.4	5.3
$q\bar{q}\mu\bar{\nu}_\mu$	0.8	4.5	0.1	1.0	0.0	0.0	6.4
$q\bar{q}\tau\bar{\nu}_\tau$	10.0	$16^{(a)}$	0.4	0.9	1.5	3.5	32

Table 2: Details of the background contaminations in the $q\bar{q}e\bar{\nu}_e$, $q\bar{q}\mu\bar{\nu}_\mu$ and $q\bar{q}\tau\bar{\nu}_\tau$ samples. Note(a): the cross contamination from other $q\bar{q}\ell\bar{\nu}_\ell$ decays to the $q\bar{q}\tau\bar{\nu}_\tau$ channel is shown for information, but as explained in the text this is not considered as background.

Source	Error
Jet reconstruction	0.16
MC statistics	0.04
W mass and LEP beam energy	0.24
Overall normalisation	0.06
MC generator	0.10
Acceptance variation	0.15
Background	0.02
Total systematics	0.35
Data statistics	$^{+0.73}_{-0.61}$

Table 3: Contributions to the error on $\alpha_{W\phi}$

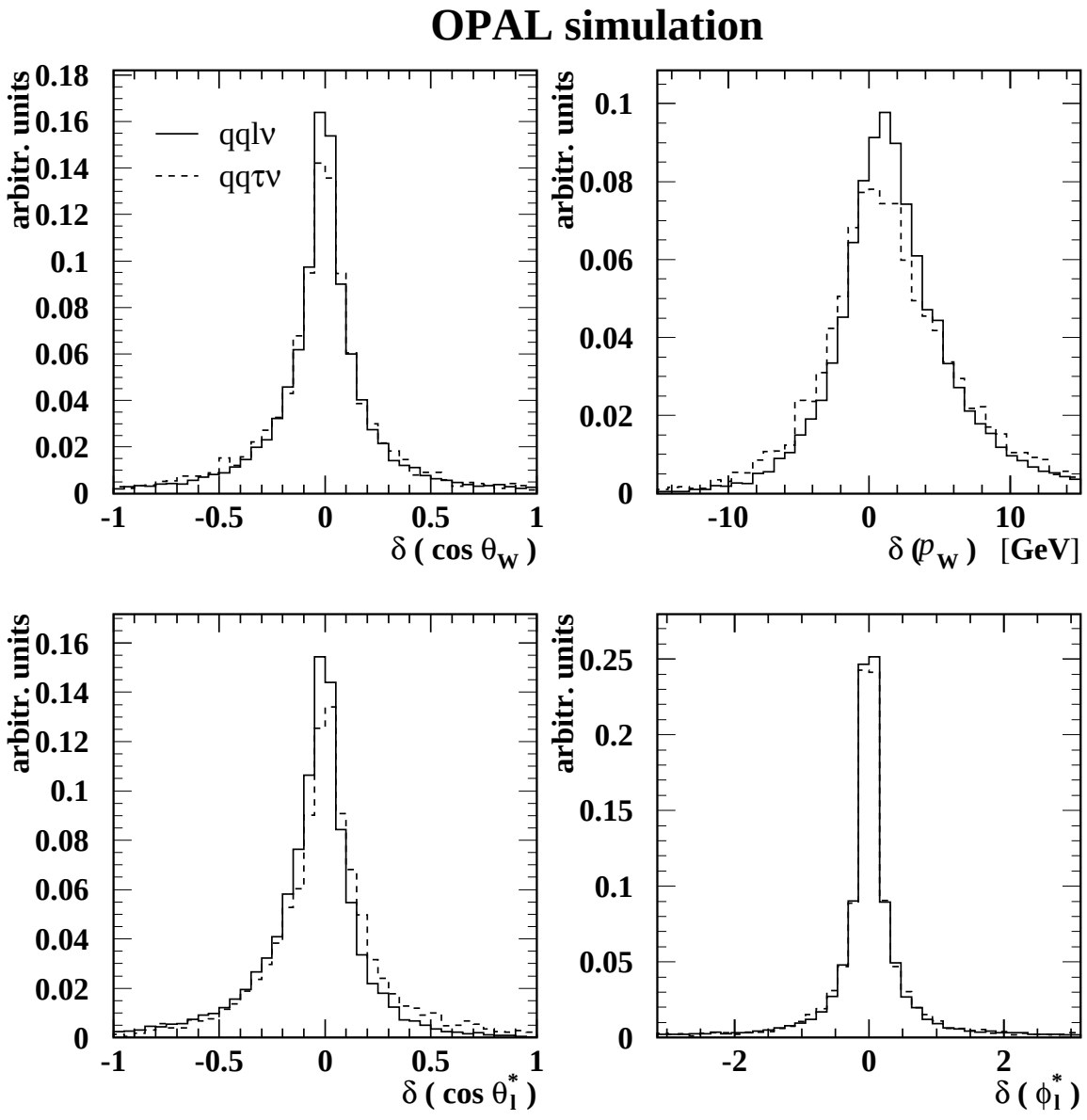

Figure 1: The resolution of the kinematic variables from the $q\bar{q}\ell\bar{\nu}_\ell$ events. All distributions show the difference between reconstructed and generated quantities. The solid line is for $q\bar{q}e\bar{\nu}_e$ and $q\bar{q}\mu\bar{\nu}_\mu$ events and the dashed line is for $q\bar{q}\tau\bar{\nu}_\tau$ events.

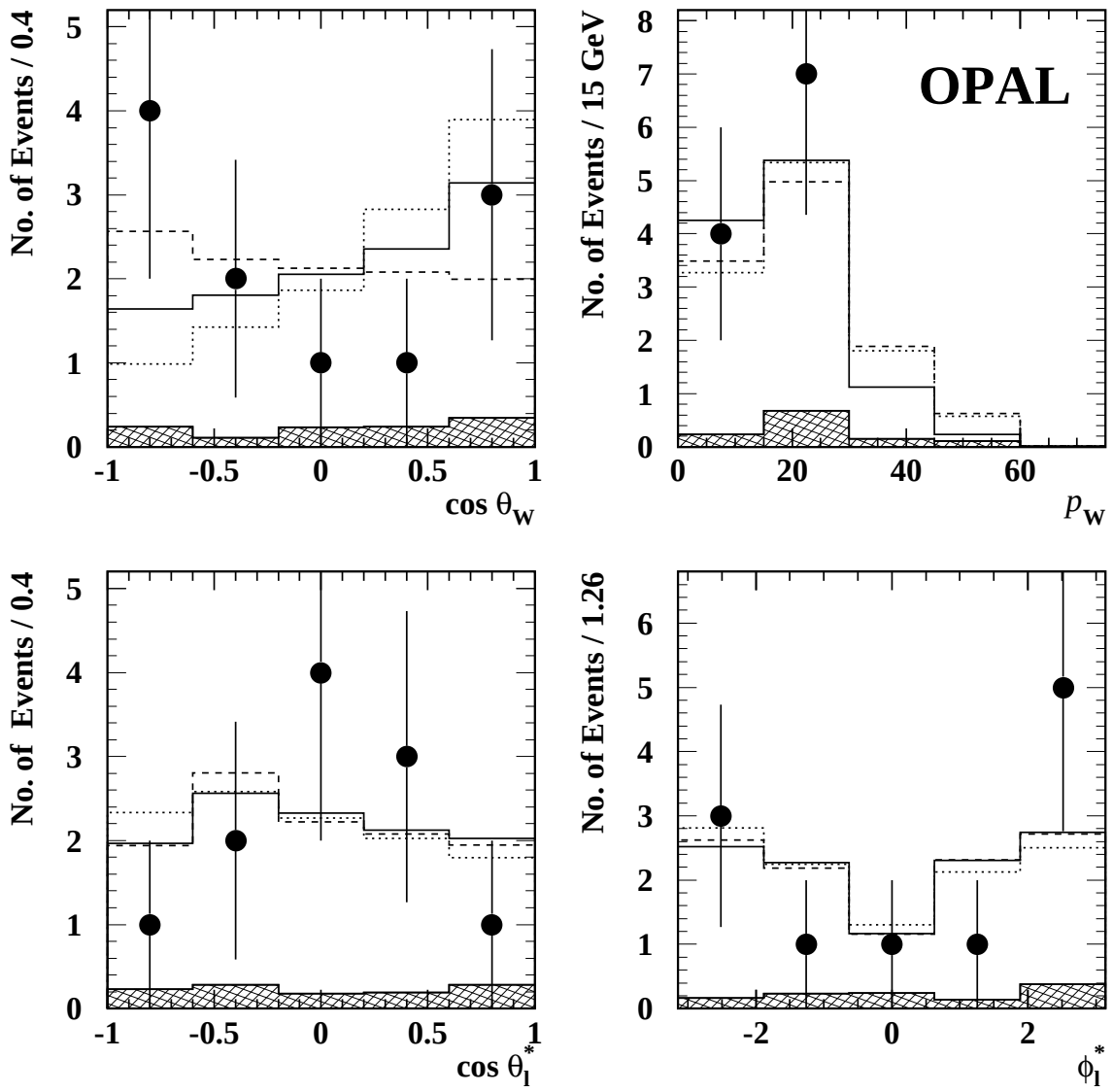

Figure 2: The distributions of $\cos\theta_{\rm W}$, $p_{\rm W}$, $\cos\theta^*_\ell$ and ϕ^*_ℓ obtained from the eleven $\rm q\overline{q}\ell\overline{\nu}_\ell$ events selected from the data. The hatched histogram shows the non $\rm q\overline{q}\ell\overline{\nu}_\ell$ background. These are compared with the distribution expected in the Standard Model using fully simulated Monte Carlo events. The predicted distributions for $\alpha_{W\phi} = +2(-2)$ are also shown as dotted (dashed) lines. Note: in the case of $\rm W^+ \to \bar{l}\nu$ events the value of ϕ^* is shifted by π in order to overlay distributions in the same plot.

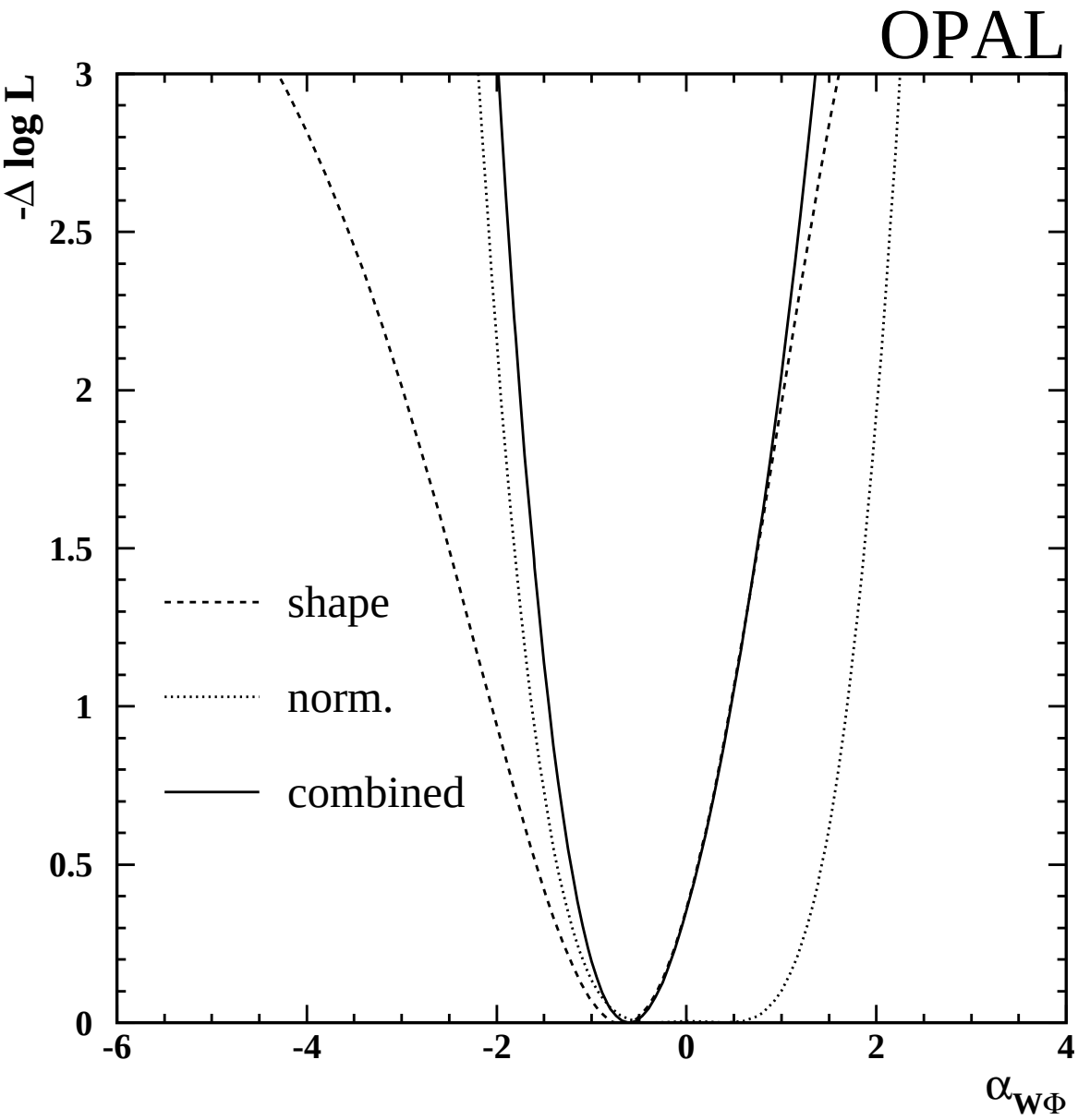

Figure 3: Likelihood distributions obtained from the cross-section (dotted) and differential distributions (dashed). The solid line is the distribution obtained by adding these together. In all cases the minimum value of the negative log likelihood has been subtracted.